



HAL
open science

Motion of the triple contact line

Vadim Nikolayev

► **To cite this version:**

Vadim Nikolayev. Motion of the triple contact line. 17e Congrès Français de Mécanique, 2005, Troyes, France. pp.1-6. hal-04275393

HAL Id: hal-04275393

<https://hal.science/hal-04275393>

Submitted on 8 Nov 2023

HAL is a multi-disciplinary open access archive for the deposit and dissemination of scientific research documents, whether they are published or not. The documents may come from teaching and research institutions in France or abroad, or from public or private research centers.

L'archive ouverte pluridisciplinaire **HAL**, est destinée au dépôt et à la diffusion de documents scientifiques de niveau recherche, publiés ou non, émanant des établissements d'enseignement et de recherche français ou étrangers, des laboratoires publics ou privés.

Motion of the triple contact line

Vadim S. Nikolayev

ESEME, Service des Basses Températures, CEA Grenoble
 Adresse postale : CEA-ESEME, PMMH, ESPCI, 10, rue Vauquelin, 75231 Paris Cedex 5
 email : vnikolayev@cea.fr

Résumé :

Dans cet exposé la cinétique de la ligne triple de contact liquide gaz solide en présence de défauts de surface est discutée. Le piégeage de la ligne triple par des défauts est analysé. On montre en quoi le piégeage de la ligne triple est différent du piégeage de la surface entre deux phases dans des milieux aléatoires. La dépendance force–vitesse est considérée pour le cas des défauts périodiques. Elle se révèle d’être fortement non linéaire près du seuil de piégeage ainsi que pour des grandes vitesses où la force se sature.

Abstract :

We propose an equation that describes the shape of the driven contact line in dynamics in presence of arbitrary (possibly random) distribution of the surface defects. It is shown that the triple contact line depinning differs from the depinning of interfaces separating two phases ; the equations describing two these phenomena have an essential difference. The force-velocity dependence is considered for a periodical defect pattern. It appears to be strongly non-linear both near the depinning threshold and for the large contact line speeds. These nonlinearity is comparable to experimental results on the contact line depinning from random defects.

Mots-clefs :

ligne triple ; piégeage ; défauts ; mouillage

1 Introduction

Motion of interphase boundaries in a random environment remains an open problem of general interest. Much attention has been paid to the depinning transition in the systems where collective pinning creates non-trivial critical behavior of the interface separating two different phases : fluid invasion in porous media, magnetic domain wall motion, flux vortex motion in type II superconductors, charge density wave conduction, dynamics of cracks, solid friction [1, 2]. The theory of the depinning transition is based on the analysis of the following equation for the interface position h :

$$\frac{\partial h}{\partial t} = F + \eta(h) + G[h], \quad (1)$$

where F is the externally imposed force, η is the noise due to the randomness of the media, t is time, and $G[\cdot]$ is some operator. When F is close to the depinning threshold F_c (where the interface begins to move), this approach generally results in the power law for the average interface velocity $v \sim (F - F_c)^\beta$. When $F \gg F_c$, a conventional linear mobility law becomes valid.

Depinning of the triple gas-liquid-solid contact line on a solid surface with defects is another example of the depinning transition. The outlined above general approach to the interface depinning phenomena is frequently applied to the contact line depinning [3]. However, the discrepancy between the theory and the experimental data on contact line motion is notable. First,

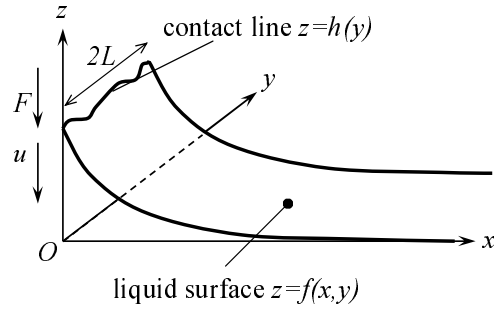


FIG. 1 – Reference system to describe the Wilhelmy balance experiment. The Wilhelmy plate is positioned in yOz plane. The positive directions for u and F are shown too.

$\beta < 1$ according to the theoretical studies while $\beta \geq 1$ is found experimentally [4]. Second, the linear mobility regime was never obtained [4]. In this paper we propose a framework suitable to explain these results.

2 Modelling of the contact line motion

Most contact line motion quasistatic models [5] result in the following expression for the contact line velocity v_n as a function of the dynamic contact angle θ :

$$v_n = \frac{\sigma}{\xi} (\cos \theta_{eq} - \cos \theta), \quad (2)$$

where θ_{eq} is the equilibrium (Young) value of the contact angle, σ is the surface tension, and ξ is a mechanism-dependent coefficient that has the same dimension as the shear viscosity μ .

The equation for the spontaneous motion has been derived in [6]. In this paper we deal with the Wilhelmy geometry (Fig. 1), where the vertical plate with surface defects can be moved up and down with a constant velocity u ($u > 0$ for the advancing contact line is assumed).

The account of the gravity influence permits [6] to avoid logarithmic divergences and thus obtain the contact line profile.

The average value of the force F exerted on this plate due to the presence of the moving contact line can be measured with a high precision [4]. The liquid-gas interface is assumed to be described by the function $z = f(x, y, t)$ where t is time and

$$|\nabla f| \ll 1 \quad (3)$$

is assumed. The position of the contact line is then given by its height $h = h(y, t)$ such that $h(y) = f(x = 0, y)$. From now on, we omit the argument t .

Under the assumption (3), the minimization of the potential energy U of the liquid with respect to f results [6] in the following expression :

$$f = \frac{1}{2L} \sum_{n=-\infty}^{\infty} \exp\left(-x\sqrt{l_c^{-2} + \pi^2 n^2 / L^2}\right) \int_{-L}^L dy' h(y') \cos \frac{\pi n(y - y')}{L}, \quad (4)$$

where $l_c = \sqrt{\sigma/\rho g}$ is the capillary length, ρ is the liquid density and g is the gravity acceleration. We assume that f is periodic (period $2L$) in the y -direction perpendicular to the direction of

u . Following [7, 8], the surface defects are modelled by the spatial variation of the equilibrium value of the contact angle $\theta_{eq}(y, z)$ along the plate.

The contact line velocity with respect to the solid reads $v_n = \dot{h} + u$. Taking into account the expression for the dynamic contact angle θ obtained under the condition (3),

$$\cos \theta = -\partial f / \partial x|_{x=0}, \quad (5)$$

one obtains from Eq. (2) the following governing equation for h

$$\dot{h}(y) + u = \frac{\sigma}{\xi} \left\{ c[y, h(y) + ut] - \frac{1}{2L} \sum_{n=-\infty}^{\infty} \sqrt{l_c^{-2} + \pi^2 n^2 / L^2} \int_{-L}^L dy' h(y') \cos \frac{\pi n(y - y')}{L} \right\}, \quad (6)$$

where $c(y, z) = \cos[\theta_{eq}(y, z)]$ is introduced for brevity.

One can easily derive a simpler "long-wave limit" version of Eq. (6) by expanding $h(y')$ around $h(y)$ in the Taylor series and tending $L \rightarrow \infty$:

$$\dot{h} + u = \frac{\sigma}{\xi} \left[c(y, h + ut) - \frac{h}{l_c} + \frac{l_c}{2} \frac{\partial^2 h}{\partial y^2} \right]. \quad (7)$$

Notice that Eqs. (6,7) have the form (1), where the random term η is replaced by the random term c . However, the external force F is missing.

3 External force

The additional force F that acts on the Wilhelmy plate due to the presence of the contact line (per unit plate width in y -direction) consists of two parts [9] : the contribution of the interface tensions at the contact line and the "friction" force due to the energy dissipation :

$$F = \frac{1}{2L} \int_{-L}^L dy \left\{ \sigma_{LS} - \sigma_{GS} + \xi \left[\dot{h}(y) + u \right] \right\}, \quad (8)$$

where the surface tensions of the gas-solid (σ_{GS}) and liquid-solid (σ_{LS}) interfaces are introduced. According to the Young formula, $c(y, z) = (\sigma_{GS} - \sigma_{LS})/\sigma$. By using Eq. (2), one obtains the final expression

$$F = -\frac{\sigma}{2L} \int_{-L}^L \cos \theta(y) dy, \quad (9)$$

which means that the force in σ units at each time moment can be obtained by averaging the cosine of the dynamic contact angle along the contact line. This force can be measured directly by separating it out from viscous drag using special experimental techniques [4] and presented as a counterpart of the external force F in Eq. (1) for the case of contact line depinning.

We consider below a periodical both in the directions y and z pattern of round spots of the radius r shown in Fig. 2. Inside the spots, $\theta_{eq} = \theta_d$, the rest of the plate having $\theta_{eq} = \theta_s$.

Because of the nonlinearity in the c term, Eq. (6) seems to be complicated and difficult to solve numerically. However, both the integration and the n -summation can be performed numerically with highly efficient Fast Fourier Transform algorithm.

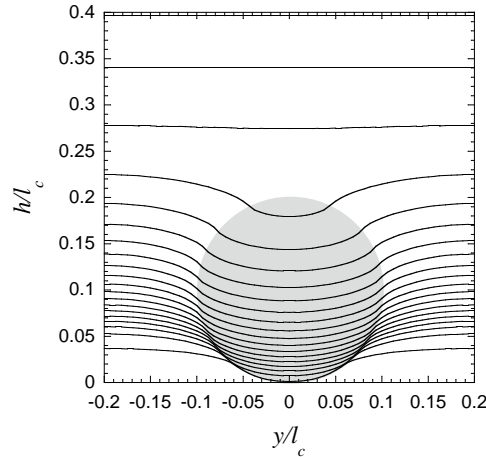


FIG. 2 – A unit cell for the periodic defect pattern (the area of a defect is shadowed) and periodic (both in *time* and space) solution of Eq. (6). 20 snapshots of the contact line with the equal time intervals $0.2\xi l_c/\sigma$ are shown for $v = 0.1\sigma/\xi$. The chosen parameters of the defect pattern are $2L = 0.4l_c$, $r = 0.1l_c$, $\theta_s = 70^\circ$, and $\theta_d = 110^\circ$. The full picture of the contact line motion can be obtained by periodic continuation of this image in both vertical and horizontal directions.

We are interested in the solutions periodic both in y and t . The time periodicity is sought to obtain time averaged values independent on the initial position of the liquid surface. The time averages are denoted by the angle brackets, e.g. the average force is

$$\langle F \rangle = \frac{1}{P} \int_0^P F(t) dt, \quad (10)$$

where $P = 2L/|u|$ is the time period. The average contact line speed $v \equiv \langle v_n \rangle = u$. The time-periodic behavior appears after the contact line goes through several first rows of the defects.

An example for such a double periodic solution is shown in Fig. 2. The snapshots of the contact line are "taken" with the equal time intervals, the contact line speed can be evaluated from the density of the snapshots. One can see that when the contact line meets a line of defects, its central portion remains stuck until the whole contact line slows down to let the liquid surface accumulate its energy for the following fast slip motion.

The force (9) can be calculated using Eq. (5) for each of the $h(y)$ curves like those in Fig. 2. It is convenient to take as a reference value

$$F_{CB} = \sigma \cos \theta_{CB} - \xi v, \quad (11)$$

where $\cos \theta_{CB} = \varepsilon^2 \cos \theta_d + (1 - \varepsilon^2) \cos \theta_s$ is the Cassie-Baxter value of the static contact angle, and $\varepsilon^2 = \pi(r/2L)^2$ is the defect density. F_{CB} corresponds to a force that would be induced by a homogeneous solid with the equilibrium contact value equal to θ_{CB} which is simply a spatially averaged value of the contact angle.

The dependence of $\langle F \rangle - F_{CB}$ on v (inverted for compatibility with Fig. 3b) is shown in Fig. 3a for different defect densities ε^2 that correspond to different L values. Both advancing ($v > 0$) and receding ($v < 0$) branches are presented. The deviation of $\langle F \rangle$ from F_{CB} increases with the increasing defect density (decreasing distance between the defects) which is explained by the increasingly strong pinning. By recalling that the average cosine of the contact angle is

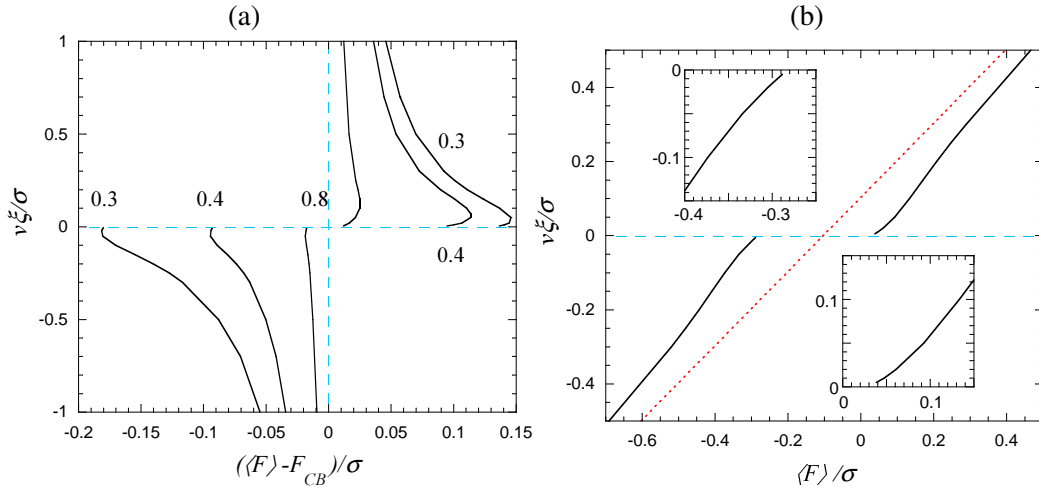


FIG. 3 – (a) $v(\langle F \rangle - F_{CB})$ curves calculated for different distances between defect centres $2L$ (shown as a curve parameter in l_c units). Both advancing ($v > 0$) and receding ($v < 0$) branches are presented. (b) $v(\langle F \rangle)$ curve for $2L = 0.3l_c$. The $v(F_{CB})$ dependence is shown as a dotted line. The portions of the curves near $v = 0$ are zoomed in the inserts. Note that the abscissa is the averaged value of $\cos \theta$. Same parameters of the defect pattern as for Fig. 2 are used.

$\langle F \rangle/\sigma$, one finds out that the cosines of the static advancing and receding contact angles (the values of $\langle F \rangle/\sigma$ at $v \rightarrow \pm 0$) also drift away from the Cassie-Baxter value with the increasing pinning.

One notices that the surface defects manifest itself much stronger at smaller velocities. It is quite a general feature : at $|v| \geq \sigma/\xi$ the contact line does not "feel" the θ_{eq} fluctuations any more and the average cosine of the dynamic contact angle is defined by $\cos \theta_{CB} - \xi v/\sigma$ for any defect pattern until it attains the saturation regime at $\cos \theta \approx \pm 1$. Unfortunately, we are unable to see this saturation of $|F|$ at the σ value : $|F| \ll \sigma$ was implicitly assumed during the derivation of Eqs. (6,7).

The decreasing slope of the $v(F)$ curve at $F \rightarrow F_c$ (that appears due to the influence of defects when $\beta > 1$) can explain the extremely slow relaxation observed during the coalescence of sessile drops [10, 11]. In this case a very small force F was imposed by the surface tension. Since the effective dissipation coefficient was inferred from the $v(F)$ slope value (inversely proportional to it), it appeared to be very large while the actual ξ value could be much smaller.

4 Conclusions

It was demonstrated in this paper that the descriptions of the depinning of interface separating two phases (e.g. for fluid invasion of porous media) and of the triple contact line, while similar in many respects, has essential differences. The main of them is related to the external force that can be controlled directly for the case of interface depinning and enters its equation of motion as an additive term. An external force can hardly be imposed directly to the triple contact line and thus does not enter its equation of motion. The experimentally measured force associated with the contact line motion can be calculated and turns out to be essentially nonlinear in the contact line velocity. At small velocities, the nonlinearity is due to the collective pinning at the surface defects, while at large velocities the force per unit contact line length is bounded by

the value of the surface tension. Our theoretical results obtained for a periodical defect pattern suggest that the experimentally observed [4] nonlinearity of the force-velocity curve is a result of the collective pinning on the defects rather than a consequence of their randomness.

The equations of the contact line motion are derived. They can be applied to analyze the collective effect of surface defects on the contact line motion for random defect patterns.

The author would like to thank E. Rolley, S. Moulinet for useful discussions and D. Beysens for numerous fruitful discussions and friendly support.

Références

- [1] A.-L. Barabási and H.E. Stanley. *Fractal Concepts in Surface Growth*. Cambridge University Press, Cambridge, 1995.
- [2] Daniel S. Fisher. Collective transport in random media : from superconductors to earthquakes. *Phys. Rep.*, 301 :113 – 150, 1998.
- [3] D. Ertaş and M. Kardar. Critical dynamics of contact line depinning. *Phys. Rev. E*, 49(4) :R2532 – R2535, 1994.
- [4] S. Moulinet, C. Guthmann, and E. Rolley. Dissipation in the dynamics of a moving contact line : effect of the substrate disorder. *European Phys. J. B*, 37 :127 – 136, 2004.
- [5] E. Ramé. Moving contact line problem : state of the contact angle boundary condition. In A. T. Hubbard, editor, *Encyclopedia of Surface and Colloid Science*. Marcel Dekker, New York, 2002.
- [6] V. S. Nikolayev and D. A. Beysens. Equation of motion of the triple contact line along an inhomogeneous surface. *Europhysics Lett.*, 64(6) :763 – 768, 2003.
- [7] Y. Pomeau and J. Vannimenus. Contact angle on heterogeneous surfaces : weak heterogeneities. *J. Colloid Interf. Sci.*, 104(2) :477 – 488, 1984.
- [8] L. W. Schwartz and S. Garoff. Contact angle hysteresis on heterogeneous surfaces. *Langmuir*, 1 :219 – 230, 1985.
- [9] J. F. Joanny and M. O. Robbins. Motion of a contact line on a heterogeneous surface. *J. Chem. Phys.*, 92 :3206 – 3212, 1990.
- [10] C. Andrieu, D. A. Beysens, V. S. Nikolayev, and Y. Pomeau. Coalescence of sessile drops. *J. Fluid Mech.*, 453 :427 – 438, 2002.
- [11] R. Narhe, D. Beysens, and V. Nikolayev. Contact line dynamics in drop coalescence and spreading. *Langmuir*, 20 :1213 – 1221, 2004.